Soy Isoflavones Promote Radioprotection of Normal Lung Tissue by Inhibition of Radiation-Induced Activation of Macrophages and Neutrophils

Lisa M. Abernathy, PhD,,† Matthew D. Fountain, MS,*,† Shoshana E. Rothstein, BS,† John M. David, MD†, Christopher K. Yunker, BS,† Joseph Rakowski, PhD,† Fulvio Lonardo, MD,‡ Michael C. Joiner, PhD,† and Gilda G. Hillman, PhD*,†*

Introduction: Radiation therapy for lung cancer is limited by toxicity to normal lung tissue that results from an inflammatory process, leading to pneumonitis and fibrosis. Soy isoflavones mitigate inflammatory infiltrates and radiation-induced lung injury, but the cellular immune mediators involved in the radioprotective effect are unknown.

Methods: Mice received a single dose of 10 Gy radiation delivered to the lungs and daily oral treatment of soy isoflavones. At different time points, mice were either processed to harvest bronchoalveolar lavage fluid for differential cell counting and lungs for flow cytometry or immunohistochemistry studies.

Results: Combined soy and radiation led to a reduction in infiltration and activation of alveolar macrophages and neutrophils in both the bronchoalveolar and lung parenchyma compartments. Soy treatment protected $F4/80^{+}CD11c^{-}$ interstitial macrophages, which are known to play an immunoregulatory role and are decreased by radiation. Furthermore, soy isoflavones reduced the levels of nitric oxide synthase 2 expression while increasing arginase-1 expression after radiation, suggesting a switch from proinflammatory M1 macrophage to an anti-inflammatory M2 macrophage phenotype. Soy also prevented the influx of activated neutrophils in lung caused by radiation.

Conclusions: Soy isoflavones inhibit the infiltration and activation of macrophages and neutrophils induced by radiation in lungs. Soy isoflavones-mediated modulation of macrophage and neutrophil responses to radiation may contribute to a mechanism of resolution of radiation-induced chronic inflammation leading to radioprotection of lung tissue.

Key Words: Radiation, Soy isoflavones, Lung inflammation, Macrophages, Neutrophils.

(*J Thorac Oncol.* 2015;10: 1703–1712)

*Department of Immunology and Microbiology, †Division of Radiation Oncology, Department of Oncology, and ‡Department of Pathology, Wayne State University School of Medicine, Detroit, Michigan.

Disclosure: The authors declare no conflict of interest.

Address for correspondence: Gilda G. Hillman, PhD, Radiation Oncology Division, Department of Oncology, Wayne State University School of Medicine, Karmanos Cancer Institute, Hudson Webber Cancer Research Center, room 515, 4100 John R., Detroit, MI 48201. E-mail: hillmang@karmanos.org

DOI: 10.1097/JTO.0000000000000677

ISSN: 1556-0864/15/1012-1703

The primary goal of combining a drug modality with radiation therapy is to maximize therapeutic benefit while mitigating severe off-target side effects in the treatment of patients with cancer. Radiation injury to normal lung parenchyma is a major concern in non–small-cell lung cancer (NSCLC). Radiotherapy given concurrently with chemotherapy is the conventional treatment for locally advanced NSCLC presenting as unresectable, stage III disease in approximately 50,000 Americans per year. There is an associated overall 5-year survival rate of 20%, emphasizing the need to improve the therapeutic ratio of concurrent chemoradiotherapy.[1,2] High-intensity radiotherapy could be more effective but is limited by lung tissue toxicity presenting as radiation pneumonitis that develops in up to 30% of patients after thoracic radiation.[3,4] Radiation pneumonitis is caused by an early inflammatory process triggered by damage to lung parenchyma, epithelial cells, vascular endothelial cells, and stroma. This process involves induction of proinflammatory cytokines and chemokines, which recruit inflammatory immune cells to the lung tissue resulting in pneumonitis and late fibrosis.[5–7] Early acute pneumonitis occurs by 2 to 4 months after radiotherapy, whereas late chronic pneumonitis manifests clinically over 6 to 24 months.[3,4] At late stages, radiation-induced pulmonary fibrosis results from aberrant resolution of inflammation in contrast to classic wound-healing processes.[6] These adverse events after radiotherapy affect patients' breathing and their quality of life. Various strategies to decrease the extent of pneumonitis have been investigated but need further research efforts.[8]

We previously explored a complementary approach to alleviate lung radiation toxicity using soy isoflavones, consisting of genistein, daidzein, and glycitein phytoestrogens extracted from soy beans. Although these isoflavones are similar in their chemical structure to estrogens, they have weak estrogenic activity and act as chemopreventive agents.[9–11] Our studies demonstrated that soy isoflavones have the dual capability of protecting normal lung from radiation injury and simultaneously enhancing radiation damage in the malignancy.[12,13] Soy mitigated the vascular damage, inflammation, and fibrosis caused by radiation injury to lung tissue in a lung cancer model suggesting that soy can alter the radiation-induced inflammatory response.[12,13] In naive mice,

soy isoflavones supplementation given prethoracic and postthoracic radiation protected the lungs against adverse effects of radiation including skin injury, hair loss, increased breathing rates, inflammation, pneumonitis, and fibrosis.[14] These findings in naive mice corroborated our findings in lung tumor models and provided evidence for a radioprotective effect of soy isoflavones. Importantly, soy isoflavones also sensitized cancer cells to radiation both in vivo and in vitro in preclinical tumor models of lung cancer, demonstrating a differential effect of radioenhancement on lung tumors with simultaneous radioprotection of normal lung tissue.[12,13,15]

We have reported that supplementation of soy isoflavones with thoracic irradiation mitigates radiation-induced inflammatory cytokines, infiltration of inflammatory cells, and fibrosis,[12–14] but the cellular mediators of radioprotection remain unclear. In this study, we investigated the role of macrophages and neutrophils in the mitigation of radiation-induced inflammatory events by soy isoflavones in lung tissue. Macrophages are recruited as a first response to radiation-induced damage in the tumor microenvironment or in normal tissues.[16] Macrophages play distinct roles in the early versus late stages of inflammatory response.[17–19] Monocytes can differentiate into functionally different macrophage subsets. Inflammatory cytokines (tumor necrosis factor-α [TNF-α], granulocyte-macrophage colony-stimulating factor, interferon-γ) generate classically activated M1 macrophages that mediate acute inflammation and participate in Th1 reactions.[20] M2 macrophages can be activated by interleukin (IL)-4, IL-13, IL-10, transforming growth factor-β, or immune complexes, participate in Th2 and Treg reactions, and promote tumor growth and fibrosis.[21,22] M1 predominates during acute inflammation, and then switches to M2 during the wound-healing phase at later stages.[21] We tested whether soy influences macrophage skewing to M1 or M2 subsets, and if this altering of macrophage phenotypes could dictate normal lung response to radiation-induced damage.

Activation and infiltration of neutrophils are a hallmark event in the progression of acute lung injury[23] and have been shown to be involved in radiation-induced alveolitis.[24] Therefore, the effect of soy isoflavones on infiltration and activation status of neutrophils was studied after radiation to the lungs. Our findings suggest that soy can inhibit the infiltration and activation of macrophages and neutrophils induced by radiation in lung parenchyma. Radiation induced a proinflammatory M1 macrophage phenotype in lungs, while mice receiving soy isoflavones and radiation switched to an anti-inflammatory M2 macrophage subtype. These data indicate that soy isoflavones modulate the cellular mediators of the inflammatory response induced by radiation.

MATERIALS AND METHODS

Mice

Female BALB/c mice (Harlan, Indianapolis, IN), 5 to 6 weeks old, were housed in facilities accredited by the Association for Assessment and Accreditation of Laboratory Animal Care. The animal protocol was approved by Wayne State University Institutional Animal Care and Use Committee.

Soy Isoflavones

The soy isoflavone mixture G-4660 used is a pure extract of 98.16% isoflavones from soybeans consisting of 83.3% genistein, 14.6% daidzein, and 0.26% glycitein (manufactured by Organic Technologies (Conshocton, OH) and obtained from the National Institutes of Health [NIH], Bethesda, MD). The soy isoflavone mixture was dissolved in DMSO and mixed with sesame seed oil at a 1:20 ratio just before treatment to facilitate gavage and avoid irritation of the esophagus by DMSO.[12–14]

Lung Irradiation

Radiation was delivered to the whole lung. Three anesthetized mice, in jigs, were positioned under a 6.4-mm lead shield with three cut-outs in an aluminum frame mounted on the radiograph machine for selective irradiation of the lung, as previously described.[13] The dose rate was 101 cGy/minute, and half value layer was 2 mm Cu. Photon irradiation was performed at a dose of 10 Gy with a Siemens Stabilipan X-ray set operated at 250 kV, 15 mA with 1-mm copper filtration at a distance of 47.5 cm from the target.

Experimental Design

Mice were pretreated with oral soy isoflavones for 3 days at a dose of 5 mg/day (250 mg/kg). Then, the lung was selectively irradiated with 10 Gy. Soy treatment was continued at 5 mg/day for 10 days and then switched to a lower dose of 1 mg/day (50 mg/kg), given 5 days a week for up to 18 weeks, based on previous studies.[12,25] We have reported that these doses of soy isoflavones result in plasma levels comparable with those measured in Asian populations consuming foods rich in soy isoflavones (1–4 μM).[14] At different time points, mice were either processed to harvest bronchoalveolar lavage (BAL) fluid for differential cell counting and lungs for flow cytometry or immunohistochemistry studies.

Analysis of Immune Cells by Differential Cell Counting in BAL Fluid and Flow Cytometry on Single-cell Suspension from Lungs

BAL was performed before lung resection at 1, 8, 12, and 18 weeks after irradiation. Cells were loaded onto slides using a cytospin centrifuge and stained using a DiffQuik staining kit (IMEB Inc., San Marcos, CA,). Differential cell counts of leukocyte subsets were performed by counting at least 300 nucleated cells.[26]

After collection of BAL fluids, the same mice provided the lungs for flow cytometry studies. Lungs were digested with 0.4 mg/ml collagenase IV, and red blood cells were lysed. Lung single-cell suspensions were incubated with Fc receptor-blocking antibody (eBioscience, San Diego, CA) before staining. For morphological characterization of leukocytes, $CD45^+$ cells were sorted by fluorescence-activated cell sorting (FACS) using a BD FACSVantage SE. $CD45^+$ cell subsets were gated according to cell size and granularity. Cell subsets obtained from each gate were spun onto slides using a cytospin and stained using a DiffQuik staining kit. To determine immunophenotype, cells were immunostained using a 5-color fluorophore combination of

antibodies consisting of CD45-APC, CD11b-FITC, F4/80-PE, CD11c-APC-eFluor780, and Ly6G-PerCp-Cy5.5 (eBioscience). Fixable viability dye eFluor450 was used to exclude dead cells. Cells were analyzed by flow cytometry using a BD LSR II flow cytometer (BD Biosciences, San Jose, CA) followed by analysis on FlowJo v10 software (TreeStar, Ashland, OR).

Immunohistochemistry

Lungs were intratracheally instilled with 10% formalin, resected, embedded in paraffin, and sectioned. Sections were incubated with primary antibodies directed against F4/80, nitric oxide synthase 2 (NOS2), arginase-1 (Arg-1), Gr-1 (Ly6C/Ly6G), and myeloperoxidase (MPO) (Abcam, Cambridge, United Kingdom) followed by biotinylated secondary antibodies (Vector Labs, Burlingame, CA). Staining was amplified using the avidin–biotin immunoperoxidase technique (Vector Labs). All slides were examined on a Nikon E800 microscope. Quantitation of the number of macrophages and measurement of cell areas were performed using ImageJ software in 10 fields of 40× per slide. For quantitation of overall staining, whole slide imaging was performed using a slide scanner and DensitoQuant analysis (3D Histech, Perkin Elmer, Hopkinton, MA). The percentage of positive area was calculated as the number of positive pixels divided by total number of pixels.

Preparation of Lung Tissue Protein Lysates and Western Blot Analysis

Protein lysates were prepared from frozen lungs using a gentleMACS tissue dissociator (Miltenyi Biotec, San Diego, CA). Lung protein extracts (50 μg) were loaded and separated on 10% sodium dodecyl sulfate polyacrylamide gel electrophoresis and transferred to Whatman membranes. Membranes were incubated with anti-MPO followed by horseradish peroxidase conjugated goat-anti-rabbit secondary antibody (IgG-HRP). Membranes were reprobed with anti-β-actin Ab as a loading control, visualized by SuperSignal West Pico chemiluminescent substrate (ThermoFisher Scientific, Waltham, MA), and captured on a Fotodyne imaging system (Fotodyne Incorporated, Hartland, WI).[15]

Statistical Analysis

Comparisons between means of two treatment groups were analyzed by two-tailed unpaired Student's *t* test. A value of p less than 0.05 was considered statistically significant.

RESULTS

Effect of Radiation and Soy Isoflavones on Immune Cell Subsets Recovered from Bronchoalveolar Space

To identify the nature of inflammatory infiltrates in lungs induced by radiation and the effect of soy isoflavones on these cells, we first analyzed immune cell subsets recovered from BAL.[26] Alveolar macrophages constituted 80% to 90% of cells recovered from BAL fluids, and the majority presented as small macrophages in both control and soy-treated BAL (Fig. 1). At 1 week after radiation, there was a significant decrease from $90.7 \pm 0.8\%$ to $24.1 \pm 2.9\%$ in small macrophages compared with control ($p < 0.0001$). A concomitant significant increase from $9.1 \pm 0.7\%$ to $75.8 \pm 3.0\%$ in enlarged foamy macrophages ($p < 0.0001$) with a structure typical of activated macrophages was observed (Fig. 1*A*, inset). This trend was consistent at 8, 12, and 18 weeks after radiation (Fig. 1*B–D*). At 8, 12, and 18 weeks after radiation and soy, there was a significant increase in small macrophages associated with a concomitant decrease in enlarged foamy macrophages ($p < 0.01$) with ratios comparable with those of control mice.

Whereas BAL fluids from control mice have undetectable numbers of neutrophils and lymphocytes, neutrophil counts showed a significant increase induced by radiation at 12 weeks ($19.0 \pm 2.1\%$, $p < 0.0001$), which was decreased in radiation and soy isoflavones–treated mice ($8.4 \pm 3.2\%$, $p < 0.05$) (Fig. 1*C*). A measurable increase in BAL lymphocytes was also observed after radiation; however, this increase was not seen in radiation and soy–treated mice.

Flow Cytometry Phenotypic Analysis of Immune Myeloid Cells Infiltrating Lung Parenchyma after Treatment with Radiation and Soy Isoflavones

Analysis of the bronchoalveolar compartment revealed that radiation caused a switch from nonactivated to activated macrophages at 2 to 4 months after radiation, which was prevented by soy isoflavones. To further determine the immunophenotype of the cells involved in the soy radioprotection, we have analyzed immune cell subsets in the lung parenchyma compartment by flow cytometry.

In a first step, lung cell suspensions from control mice were stained with anti-CD45 to separate and sort leukocytes by FACS. Gate G1 contained lymphocytes, gate G2 consisted of a majority of neutrophils/granulocytes and a few macrophages, and gate G3 was primarily composed of alveolar macrophages and some granulocytes (Fig. 2*A*). Consistent with findings in BAL, lymphocytes in gate G1 did not show major alterations by treatment (personal communications, Abernathy and Hillman); therefore, we focused on myeloid cells.

To analyze the phenotype of myeloid cells obtained from lungs at 12 weeks after radiation, cells were immunostained for CD45, CD11b, F4/80, CD11c, and Ly6G. Gates for $CD45^+$ leukocytes were set as shown in Figure 2*A*, and myeloid cells from gates G2 and G3 were further analyzed for specific macrophages and neutrophil markers. Macrophages were gated based on differential expression of F4/80 and CD11c to analyze interstitial macrophages ($F4/80^+CD11c^-$) and alveolar macrophages (AM, $F4/80^+CD11c^+$) (Fig. 2*B*).[27] Percentages of $F4/80^+CD11c^-$ interstitial macrophages subsets showed a significant decrease in interstitial macrophages induced by radiation compared with control ($p < 0.05$), whereas this treatment with soy isoflavones protected this population in irradiated lung tissue ($p < 0.05$) (Fig. 2*B*). $F4/80^+CD11c^+$ AM subsets did not show difference between treatments (Fig. 2*B*), in contrast to BAL findings that showed an increase in AM by radiation and decrease by radiation + soy. The discrepancies between alveolar macrophages in BAL fluid and lung tissue compartments could be because of lavage of loose alveolar macrophages and subsequent processing of lungs

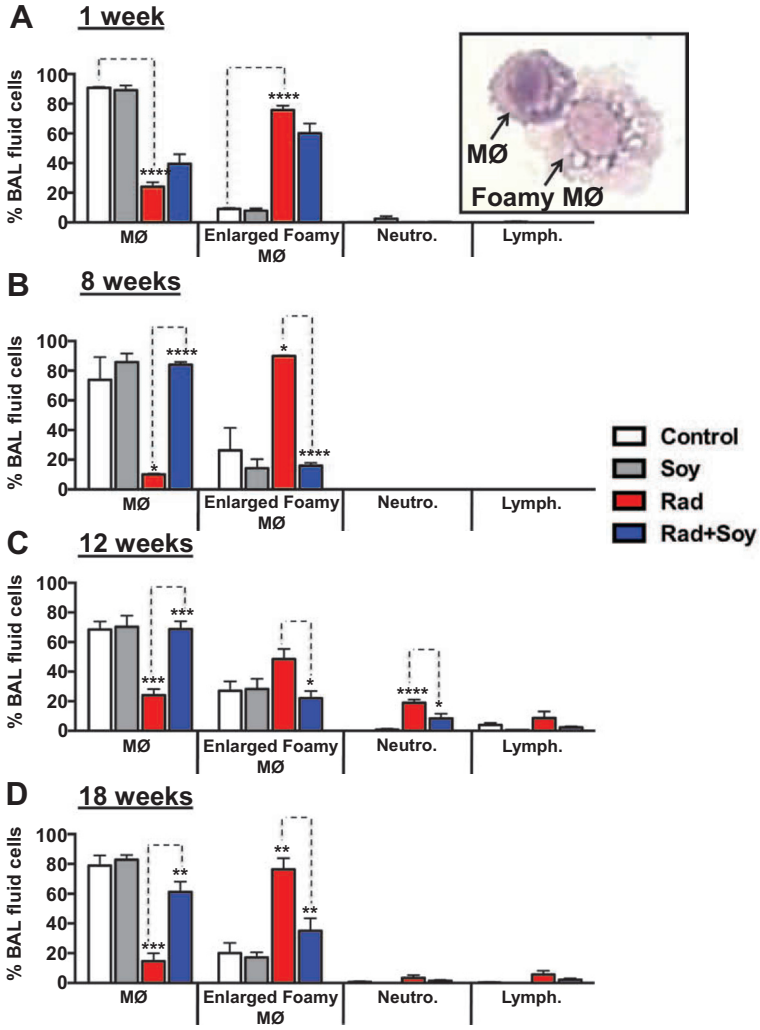

FIGURE 1. Effect of soy isoflavones on immune cells obtained from bronchoalveolar lavage (BAL) fluid at different time points after radiation. BAL fluids were harvested at early and late time points after radiation. At 1 week (*A*), 8 weeks (*B*), 12 weeks (*C*), and 18 weeks (*D*) BAL postradiation, differential cell counts on BAL fluid cytospins were performed, and the percentages of macrophages, neutrophils, and lymphocytes were calculated. The ratios of nonactivated macrophages and enlarged, foamy activated macrophages (see inset in *A*), as well as those of neutrophils and lymphocytes, are shown from BAL fluid obtained from treated and control mice. The data are presented as mean ± standard error of the mean (n = 3–5 mice/group/time point), and *p* values shown represent significant differences between radiation + soy compared with radiation alone. *$p < 0.05$, **$p < 0.01$, ***$p < 0.001$, ****$p < 0.0001$, radiation compared with control or radiation + soy compared with radiation alone.

for FACS. Neutrophils were gated by expression of CD11b and Ly6G/Gr-1 markers within the CD45$^+$ population (Fig. 2*C*).[28] CD11b$^+$Ly6G$^+$ neutrophils in lungs are significantly increased after radiation compared with control ($p = 0.01$); however, supplementation of soy to radiation did not significantly change the percent of neutrophils (Fig. 2*C*).

Skewing Toward Anti-inflammatory M2 Macrophage Phenotype in Lung Tissue Treated with Radiation and Soy

To further study whether soy inhibits the activation of macrophages induced by radiation, as suggested in the BAL studies, we investigated macrophage subsets and their functional status in lungs treated with radiation only and radiation + soy. Radiation caused a striking infiltration of F4/80$^+$ macrophages that was prominent at 18 weeks after radiation and observed in areas of thickened alveolar septa, reflective of pneumonitis[12–14] (Fig. 3*A*, arrowheads). Numerous alveolar macrophages were particularly enlarged with abundant cytoplasm showing the structure of activated macrophages compared with small macrophages in control lungs (Fig. 3*A*, see arrows and inset). Lungs from mice treated with radiation + soy had a lower density of F4/80$^+$ macrophages and thinner alveolar septa (Fig. 3*A*), compared with radiation-treated lungs, showing decreased pneumonitis.[13,14] Moreover, the morphology of the alveolar macrophages was much smaller than those of radiation-treated lungs (see insets, Fig. 3*A*). Quantitation of F4/80$^+$ cells showed that there was a significant increase in the number of alveolar macrophages in lungs treated with radiation compared with those in control lungs ($p < 0.001$, Fig. 3*B*). Irradiated mice supplemented with soy isoflavones showed a significantly reduced number of alveolar macrophages compared with radiation alone ($p < 0.001$, Fig. 3*B*), to levels similar to those of control mice. Measurements of the average size of the alveolar macrophages showed that radiation increased the size of these cells significantly compared with either radiation + soy ($p < 0.01$, Fig. 3*C*) or control ($p < 0.0001$, Fig. 3*C*).

To further clarify the functional phenotype of infiltrating macrophages, the NOS2 activation marker for M1 macrophages and Arg-1 activation marker for M2 macrophages

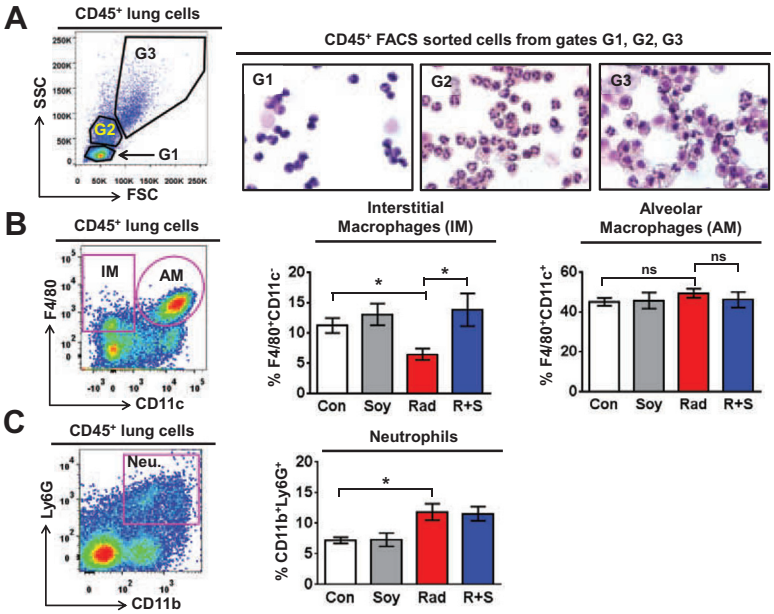

FIGURE 2. Flow cytometry analysis of macrophages and neutrophils isolated from lung tissues. *A,* Structure of FACS-sorted CD45$^+$ immune cell subsets in normal lung tissue. Normal lungs from untreated mice were dissociated into single-cell suspensions. Cells were immunostained with fluorescent anti-CD45 and sorted by FACS. CD45$^+$ lung leukocyte subsets were gated in gates G1, G2, and G3 based on cell size (forward scatter [FSC], *x*-axis) and granularity (side scatter [SSC], *y*-axis). Cells in each gate were sorted by FACS, cytospun onto slides, and stained with DiffQuik, revealing that gate G1 contained lymphocytes, gate G2 consisted of a majority of neutrophils/granulocytes and fewer macrophages, and gate G3 was primarily composed of alveolar macrophages and some granulocytes. All magnifications are at 40×. *B,* Interstitial and alveolar macrophages analysis. At 12 weeks after radiation, lungs from control (Con) mice and mice treated with soy (Soy), radiation (Rad), or radiation + soy (R + S) were dissociated into single-cell suspensions. Cells were stained with anti-CD45, anti-F4/80, and anti-CD11c fluorescent antibodies to analyze interstitial (F4/80$^+$CD11c$^-$) and alveolar (F4/80$^+$CD11c$^+$) tissue macrophages within CD45$^+$ leukocyte populations by flow cytometry. Representative flow cytometry plots are presented, showing the gating strategy of CD45$^+$ myeloid lung cells for analysis of F4/80$^+$CD11c$^-$ interstitial macrophages (in pink rectangle gate) and F4/80$^+$CD11c$^+$ alveolar macrophage (AM in pink circle gate). Percentages of F4/80$^+$CD11c$^-$ interstitial macrophages subsets and F4/80$^+$CD11c$^+$ AM subsets within CD45$^+$ cells are shown for lungs from control and treated mice. The data are presented as mean ± standard error of the mean (n = 4–5 mice/group) and are representative of three separate experiments. *C,* Analysis of CD45$^+$CD11b$^+$Ly6G$^+$ neutrophils. Cells were stained with fluorescent anti-CD45, anti-CD11b, and anti-Ly6G to analyze neutrophil subsets by flow cytometry. Representative flow cytometry plots are presented, showing the gating strategy for analysis of CD11b$^+$Ly6G$^+$ neutrophils within CD45$^+$ leukocyte populations. Percentages of CD11b$^+$Ly6G$^+$ neutrophils within CD45$^+$ cells are shown for lungs from control and treated mice. The data are presented as mean ± standard error of the mean (n = 5 mice/group) and are representative of two separate experiments. *$p < 0.05$, radiation compared with control or radiation + soy compared with radiation alone.

were used to differentiate between proinflammatory M1 macrophage phenotype and anti-inflammatory M2 macrophage phenotype. Radiation caused a prominent increase in NOS2 staining of lung tissue by 18 weeks after radiation (Fig. 4*A*), which was apparent in enlarged alveolar macrophages (Fig. 4*A*, inset). These findings were confirmed by slide scanning quantitation for the level of staining (Fig. 4*B*). In contrast, a lower level of NOS2 staining was observed after radiation + soy (Fig. 4*A*, *B*). Staining of lungs with Arg-1 showed a prominent increase in radiation + soy–treated lungs compared with radiation alone (Fig. 4*C*, *D*).

Radiation caused an increase in proinflammatory M1 macrophage phenotype defined by high NOS2 and low Arg-1 levels at 18 weeks after radiation (Fig. 4*A*, *B*). This is in contrast to relatively low NOS2 levels and high Arg-1 levels observed in lungs treated with radiation + soy or in controls (Fig. 4*B*, *C*).

Radiation-induced Infiltration and Activation of Granulocytes/Neutrophils in Lung Tissue is Decreased by Soy Isoflavones

Analysis of BAL immune cells showed an increase in neutrophils by 12 weeks after radiation. Granulocyte/neutrophil phenotype and function were determined by immunohistochemistry staining of lung tissue sections for Gr-1 (Ly6C/Ly6G) and the neutrophil marker NIMP at 12 weeks after radiation. Radiation caused a pronounced increase in clusters of Gr-1$^+$ granulocytes in areas of thickened septa at 12 weeks after radiation (Fig. 5, see inset). In contrast, following radiation + soy treatment, the alveolar septa were not as thickened and contained much lower levels of Gr-1$^+$ cells (Fig. 5). Staining of lung tissue for the neutrophil specific marker NIMP revealed the same histological patterns, with increased neutrophil infiltrates induced by radiation and decreased by radiation + soy (Fig. 5).

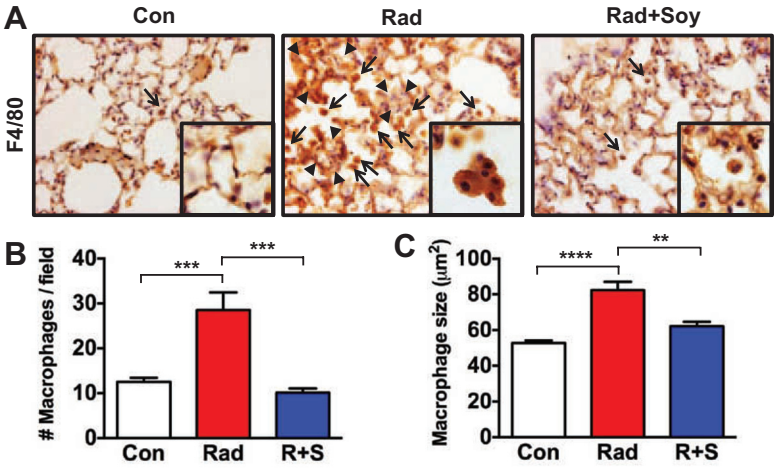

FIGURE 3. Alveolar macrophages in lungs treated with radiation and soy isoflavones at 18 weeks after radiation. Lung tissue sections were obtained from control (Con) mice and mice treated with radiation (Rad) or radiation + soy (R + S) at 18 weeks after radiation. Sections were stained by immunohistochemistry for the marker F4/80 to detect alveolar macrophages in the lungs. Arrows indicate positive staining of F4/80⁺ alveolar macrophages. *A*, Radiation caused a marked increase in macrophages in thickened alveolar septa areas (arrowheads). Numerous alveolar macrophages were particularly enlarged with abundant cytoplasm showing the structure of activated macrophages compared with small macrophages in control lungs (see inset). The density of F4/80⁺ macrophages was much lower in radiation + soy–treated lungs at 18 weeks after radiation than in radiation-treated lungs. Alveolar macrophages were smaller, resembling those of control lungs (see inset), and the architecture of the alveolar septa was thinner akin to control lung tissue showing decreased pneumonitis compared with radiation-treated lungs. *B*, Using ImageJ analysis of immunohistochemistry slides, the numbers of F4/80⁺ alveolar macrophages were counted in 10 fields of 40× per slide and the average number of F4/80⁺ cells per field ± standard error is reported for each treatment group. *C*, Measurement of the F4/80⁺ alveolar macrophage cell areas were performed using ImageJ software in 10 fields of 40× per slide and the average cell area of macrophages per field ± standard error in each treatment group is reported. The total number of macrophages counted and measured in 10 fields were 125 for control, 285 for radiation, and 101 for radiation + soy–treated mice. The means are reported in *B* and *C*. All magnifications are at 40× and insets at 100× to reveal the extent of positive staining and structure of immune cell subsets. $^{**}p < 0.01$, $^{***}p < 0.001$, $^{****}p < 0.0001$, radiation compared with control or radiation + soy compared with radiation alone.

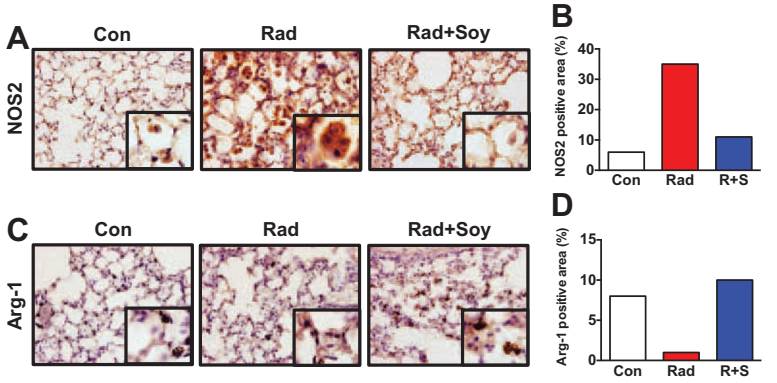

FIGURE 4. Nitric oxide synthase 2 (NOS2) and arginase (Arg)-1 functional macrophage markers in lungs treated with radiation and soy isoflavones. Lung tissue sections were obtained from control (Con) mice and mice treated with radiation (Rad) or radiation + soy (R + S) at 18 weeks after radiation. Sections were stained by immunohistochemistry for the markers NOS2 and Arg-1 to determine macrophage activation status in the lungs. *A*, NOS2 staining revealed an abundance of activated macrophages caused by radiation presenting as clusters of enlarged NOS2⁺ cells in areas of pneumonitis (see insets). Lower levels of NOS2⁺ macrophages were seen in lungs of mice treated with radiation + soy or control, which presented as smaller cells (see inset). *B*, Whole slide scanning for quantitation of NOS2 positive staining confirmed these findings. C, Compared with radiation, Arg-1 expression was greater with radiation + soy. *D*, Whole slide scanning for quantitation of revealed higher levels of Arg-1 in radiation + soy compared with low levels after radiation alone. For analysis of whole slide scanning, the percentage of positive area was calculated as the total number of positive pixels divided by total number of pixels. All magnifications are at 40× and insets at 100× to reveal the extent of positive staining and structure of immune cell subsets.

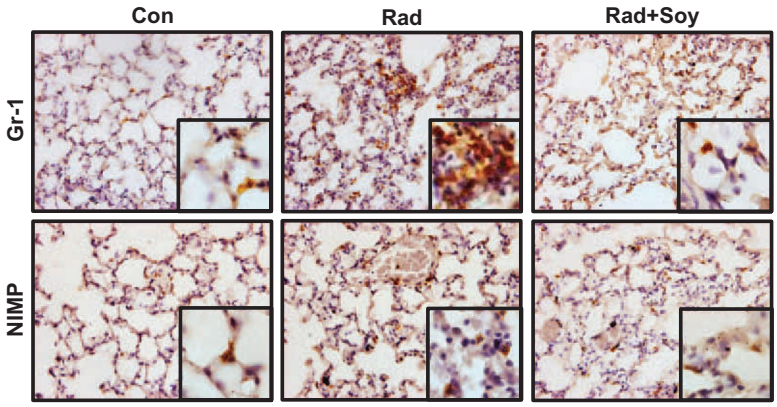

FIGURE 5. Effect of soy isoflavones on radiation-induced infiltration of granulocytes/neutrophils in lung tissue. Lungs tissue sections were obtained from control (Con) mice and mice treated with radiation (Rad) or radiation + soy (R + S) at 12 weeks after radiation. Sections were stained by immunohistochemistry for Gr-1 (Ly6C/Ly6G) and NIMP to detect granulocytes/neutrophils. Staining of Gr-1$^+$ granulocytes showed that radiation caused a pronounced increase in clusters of granulocytes in areas of thickened septa at 12 weeks after radiation (see inset). In contrast, after radiation + soy treatment, the alveolar septa were not as thickened, and much lower levels of positive cells for Gr-1 were observed. All magnifications are at 40× and insets at 100× to reveal the extent of positive staining and structure of immune cell subsets.

Concurrent with increased infiltration of Gr-1$^+$ and NIMP$^+$ cells, lungs treated with radiation also showed multiple cells with intense MPO staining (Fig. 6). MPO$^+$ cells formed clusters in areas of thickened alveolar septa, which are indicative of a massive infiltration of activated neutrophils, as confirmed by quantitative analysis of the level of positive staining (Fig. 6*A* and *B*). However, MPO$^+$ infiltrates were reduced in lungs treated with radiation + soy (Fig. 6*A* and *B*). These data indicate that radiation-induced neutrophil activation in lung tissue is inhibited by soy isoflavones. These findings were confirmed by western blot analysis of MPO expression in lung tissue lysates showing an increase induced by radiation, which was inhibited by the addition of soy isoflavones (Fig. 6*C*).

DISCUSSION

Conventional fractionated radiotherapy concurrent with chemotherapy is currently the standard of care for unresectable locally advanced NSCLC. Treatment success

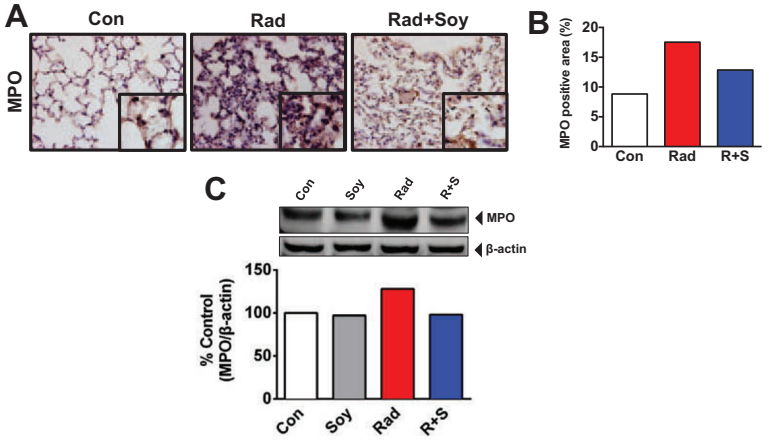

FIGURE 6. Inhibition of radiation-induced activation of neutrophils in lung tissue. Lungs tissue sections were obtained from control (Con) mice and mice treated with radiation (Rad) or radiation + soy (R + S) at 12 weeks after radiation. *A* and *B*, Sections were stained by immunohistochemistry for the neutrophil activation marker myeloperoxidase (MPO). Radiation caused extensive MPO staining in the lung tissue that is indicative of activated neutrophil infiltration. MPO$^+$ activated neutrophils were present in clusters in areas of thickened alveolar septa (see inset) at 12 weeks after radiation. The levels of MPO were greatly reduced in radiation + soy–treated lungs. *B*, Whole slide scanning for quantitation of MPO-positive staining confirmed these findings. For analysis of whole slide scanning, the percentage of positive area was calculated as the total number of positive pixels divided by total number of pixels. NIMP$^+$ neutrophils were also increased in lung tissue by radiation but not by radiation + soy. All magnifications are at 40× and insets at 100× to reveal the extent of positive staining and structure of immune cell subsets. *C*, Western blot analysis of MPO on whole tissue lysates obtained from lungs showed an increase induced by radiation, which was inhibited by the addition of soy isoflavones. Band intensities were quantified using Image J (NIH) densitometry analysis.

for this patient population has been severely constrained by pneumonitis and later fibrosis.[29,30] Hypofractionated radiotherapy is an emerging modality for early-stage lung cancer using high dose per fraction over a short time period to improve effectiveness of tumor destruction and reduce the number of visits for therapy.[31–33] However, high-intensity radiotherapy can also be associated with greater damage to lung tissue, emphasizing the need to develop complementary approaches to alleviate radiation-induced injury to normal lung structures and function.[34] Our preclinical murine studies[12–14] demonstrate that soy isoflavones can reduce the extent of inflammatory infiltrates and vascular damage caused by radiation in the lungs, suggesting that soy modulates immune responses triggered by injury. Studies on the effect of soy and the immune system in other diseases besides cancer also support this hypothesis. Genistein downregulated cytokine-induced proinflammatory pathways in human brain microvascular endothelial cells.[35] Soy isoflavones had anti-inflammatory mechanisms through modulation of leukocyte–endothelial cell interactions in the study of atherosclerosis.[36] The goals of this study were to determine whether soy isoflavones modulate innate immune cells involved in radiation-induced inflammation in normal lungs by examining the bronchoalveolar space and lung parenchyma compartments.

Macrophages are recruited as a first response to radiation-induced damage in the tumor microenvironment.[16,37] Alterations in lung macrophages after radiation have been observed during early and late phases of tissue injury[38,39] supporting the idea that macrophage activation contributes, at least partially, to the pathogenesis of radiation-induced lung injury. Therefore, modulation of the response of macrophages to radiation could be a mechanism of radioprotection by soy isoflavones. By 2 to 4 months after radiation, an increase in the number and size of macrophages was observed both in the bronchoalveolar space and lung parenchyma compartments, indicative of macrophage activation, confirming previous reports.[38,39] Soy isoflavones durably decreased the frequency and size of macrophages found in the lung after radiation.

Our flow cytometry analysis of lung parenchyma after lavage identified subsets of residual $F4/80^{+}CD11c^{+}$ alveolar macrophages and $F4/80^{+}CD11c^{-}$ interstitial macrophages, as reported by others.[40] A decrease in interstitial macrophages was induced by radiation, whereas this subset was protected by the addition of soy isoflavones. Interstitial macrophages played immunoregulatory roles in the maintenance of lung homeostasis and in pathologic conditions.[41] Soy could potentially inhibit inflammatory responses by protecting interstitial macrophages. In contrast, alveolar macrophages exhibit a greater capacity to functionally contribute to pulmonary inflammation and antimicrobial defense.[42] We found that soy isoflavones inhibited alveolar macrophage infiltration and activation induced by radiation, a possible mechanism controlling inflammatory processes. These findings suggest that soy modulation of macrophage subset functions in response to radiation may play a critical role in soy-mediated radioprotective effects in lungs.

In radiation-treated lungs, our analysis of myeloid cells showed extensive infiltration of inflammatory cells at sites of pneumonitis, consisting of macrophages and neutrophils. Both types of immune cells were morphologically and molecularly in a status of activation. In contrast, soy supplementation to radiation decreased both the infiltration and activation of myeloid cells. The influence of soy isoflavones on M1 and M2 macrophage polarization in irradiated lungs could be a mechanism of radioprotection. Macrophages possess the plasticity to respond to environmental stressors in tissues that functionally range from M1 proinflammatory to M2 immunosuppressive, anti-inflammatory phenotypes.[43,44] These two phenotypes can be distinguished by expression of NOS2 and Arg-1.[45] Normal tissue exposed to ionizing radiation generates "damage" signals and type 1 cytokines, such as IL-1β, IL-6, and TNF-α, that classically activate macrophages (M1) and drive the acute/chronic pulmonary inflammation induced by radiation.[46,47] M1 macrophages produce NOS2, which generates reactive NO species, thus promoting inflammation. Alternatively activated macrophages (M2) are important for the resolution of inflammation.[48] M2 macrophages produce Arg-1, which generates L-ornithine from arginine, which is a precursor of proline, known to enhance collagen synthesis, thus promoting tissue repair and resolution of inflammation.[43,49] Our studies now demonstrate that radiation induced a proinflammatory M1 phenotype in lungs at late time points, whereas mice receiving soy isoflavones and radiation switched to an anti-inflammatory M2 subtype with increased levels of Arg-1 and decreased NOS2. These data indicate that soy isoflavones supplementation to radiation could result in skewing of alveolar macrophages from a proinflammatory M1 phenotype toward an anti-inflammatory M2 phenotype. These data are in agreement with soy isoflavones inhibition of the release of TNF-α, IL-1β, IL-6, and interferon-γ proinflammatory cytokines induced by radiation in lung tissues that promote an M1 macrophage phenotype.[13]

Infiltration and activation of neutrophils into the lung are key factors that occur after damage to lung tissue.[23,38] Therefore, inhibition of the inflammatory neutrophil response induced by radiation in the pulmonary environment may result in reduced host tissue damage. Our flow cytometry studies of lung single-cell suspensions showed that $CD11b^{+}Ly6G^{+}$ neutrophils were increased after radiation. Immunostaining confirmed clusters of activated neutrophils, as confirmed by MPO staining, in sites of pneumonitis caused by radiation. Treatment with soy isoflavones inhibited radiation-induced neutrophil infiltration and activation, suggesting a mechanism of protection from tissue damage by soy.

In summary, our preclinical study in lung suggests that a radioprotective mechanism of soy isoflavones could involve inhibition of infiltration and activation of macrophages and neutrophils in irradiated lungs. These findings indicate that soy isoflavones used as a complementary intervention to radiotherapy for lung cancer could potentially reduce lung toxicity. This approach has been translated into an ongoing phase I clinical trial of chemoradiotherapy for advanced stage III NSCLC to evaluate the safety and efficacy of soy isoflavone supplementation.

ACKNOWLEDGMENTS

These studies were supported by the American Institute for Cancer Research grant #10A108, grant R21CA155518 from the National Cancer Institute, and a Wayne State University Boost Grant awarded to G.G.H. The content is solely the responsibility of the authors and does not necessarily represent the official views of the National Cancer Institute or National Institutes of Health. L.M.A. was supported by a Thomas C. Rumble Fellowship provided by the Graduate School at Wayne State University. The Microscopy, Imaging and Cytometry Resources Core is supported, in part, by the NIH Center grant P30 CA022453 to the Karmanos Cancer Institute at Wayne State University and the Perinatology Research Branch of the National Institutes of Child Health and Development at Wayne State University. We also thank Kali Hankerd and David Hoogstra for excellent technical assistance.

REFERENCES

1. van Meerbeeck JP, Meersschout S, De Pauw R, Madani I, De Neve W. Modern radiotherapy as part of combined modality treatment in locally advanced non-small cell lung cancer: present status and future prospects. *Oncologist* 2008;13:700–708.
2. Bradley JD, Bae K, Graham MV, et al. Primary analysis of the phase II component of a phase I/II dose intensification study using three-dimensional conformal radiation therapy and concurrent chemotherapy for patients with inoperable non-small-cell lung cancer: RTOG 0117. *J Clin Oncol* 2010;28:2475–2480.
3. Kong FM, Hayman JA, Griffith KA, et al. Final toxicity results of a radiation-dose escalation study in patients with non-small-cell lung cancer (NSCLC): predictors for radiation pneumonitis and fibrosis. *Int J Radiat Oncol Biol Phys* 2006;65:1075–1086.
4. Schallenkamp JM, Miller RC, Brinkmann DH, Foote T, Garces YI. Incidence of radiation pneumonitis after thoracic irradiation: Dose-volume correlates. *Int J Radiat Oncol Biol Phys* 2007;67:410–416.
5. Hill RP. Radiation effects on the respiratory system. *Br J Radiol* 2005;27:75–81.
6. Bentzen SM. Preventing or reducing late side effects of radiation therapy: radiobiology meets molecular pathology. *Nat Rev Cancer* 2006;6:702–713.
7. Hill RP, Zaidi A, Mahmood J, Jelveh S. Investigations into the role of inflammation in normal tissue response to irradiation. *Radiother Oncol* 2011;101:73–79.
8. Mehta V. Radiation pneumonitis and pulmonary fibrosis in non-small-cell lung cancer: pulmonary function, prediction, and prevention. *Int J Radiat Oncol Biol Phys* 2005;63:5–24.
9. Hebert JR, Hurley TG, Olendzki BC, Teas J, Ma Y, Hampl JS. Nutritional and socioeconomic factors in relation to prostate cancer mortality: a cross-national study. *J Natl Cancer Inst* 1998;90:1637–1647.
10. Kuiper GG, Lemmen JG, Carlsson B, et al. Interaction of estrogenic chemicals and phytoestrogens with estrogen receptor beta. *Endocrinology* 1998;139:4252–4263.
11. Banerjee S, Li Y, Wang Z, Sarkar FH. Multi-targeted therapy of cancer by genistein. *Cancer Lett* 2008;269:226–242.
12. Hillman GG, Singh-Gupta V, Runyan L, et al. Soy isoflavones radiosensitize lung cancer while mitigating normal tissue injury. *Radiother Oncol* 2011;101:329–336.
13. Hillman GG, Singh-Gupta V, Hoogstra DJ, et al. Differential effect of soy isoflavones in enhancing high intensity radiotherapy and protecting lung tissue in a pre-clinical model of lung carcinoma. *Radiother Oncol* 2013;109:117–125.
14. Hillman GG, Singh-Gupta V, Lonardo F, et al. Radioprotection of lung tissue by soy isoflavones. *J Thorac Oncol* 2013;8:1356–1364.
15. Singh-Gupta V, Joiner MC, Runyan L, et al. Soy isoflavones augment radiation effect by inhibiting APE1/Ref-1 DNA repair activity in non-small cell lung cancer. *J Thorac Oncol* 2011;6:688–698.
16. Gough MJ, Young K, Crittenden M. The impact of the myeloid response to radiation therapy. *Clin Dev Immunol* 2013;2013:281958.
17. Gensel JC, Zhang B. Macrophage activation and its role in repair and pathology after spinal cord injury. *Brain Res* 2015;1619:1–11.
18. Lucas T, Waisman A, Ranjan R, et al. Differential roles of macrophages in diverse phases of skin repair. *J Immunol* 2010;184:3964–3977.
19. Duffield JS, Forbes SJ, Constandinou CM, et al. Selective depletion of macrophages reveals distinct, opposing roles during liver injury and repair. *J Clin Invest* 2005;115:56–65.
20. Ricardo SD, van Goor H, Eddy AA. Macrophage diversity in renal injury and repair. *J Clin Invest* 2008;118:3522–3530.
21. Deonarine K, Panelli MC, Stashower ME, et al. Gene expression profiling of cutaneous wound healing. *J Transl Med* 2007;5:11.
22. Munder M, Eichmann K, Morán JM, Centeno F, Soler G, Modolell M. Th1/Th2-regulated expression of arginase isoforms in murine macrophages and dendritic cells. *J Immunol* 1999;163:3771–3777.
23. Grommes J, Soehnlein O. Contribution of neutrophils to acute lung injury. *Mol Med* 2011;17:293–307.
24. Haston CK, Begin M, Dorion G, Cory SM. Distinct loci influence radiation-induced alveolitis from fibrosing alveolitis in the mouse. *Cancer Res* 2007;67:10796–10803.
25. Hillman GG, Wang Y, Kucuk O, et al. Genistein potentiates inhibition of tumor growth by radiation in a prostate cancer orthotopic model. *Mol Cancer Ther* 2004;3:1271–1279.
26. De Brauwer EI, Jacobs JA, Nieman F, Bruggeman CA, Drent M. Bronchoalveolar lavage fluid differential cell count. How many cells should be counted? *Anal Quant Cytol Histol* 2002;24:337–341.
27. Bedoret D, Wallemacq H, Marichal T, et al. Lung interstitial macrophages alter dendritic cell functions to prevent airway allergy in mice. *J Clin Invest* 2009;119:3723–3738.
28. Rose S, Misharin A, Perlman H. A novel Ly6C/Ly6G-based strategy to analyze the mouse splenic myeloid compartment. *Cytometry A* 2012;81:343–350.
29. Aupérin A, Le Péchoux C, Rolland E, et al. Meta-analysis of concomitant versus sequential radiochemotherapy in locally advanced non-small-cell lung cancer. *J Clin Oncol* 2010;28:2181–2190.
30. Guida C, Maione P, Rossi A, et al. Combined chemo-radiotherapy for locally advanced non-small cell lung cancer: current status and future development. *Crit Rev Oncol Hematol* 2008;68:222–232.
31. Lo SS, Sahgal A, Chang EL, et al. Serious complications associated with stereotactic ablative radiotherapy and strategies to mitigate the risk. *Clin Oncol (R Coll Radiol)* 2013;25:378–387.
32. Soliman H, Cheung P, Yeung L, et al. Accelerated hypofractionated radiotherapy for early-stage non-small-cell lung cancer: long-term results. *Int J Radiat Oncol Biol Phys* 2011;79:459–465.
33. Videtic GM, Stephans KL. The role of stereotactic body radiotherapy in the management of non-small cell lung cancer: an emerging standard for the medically inoperable patient? *Curr Oncol Rep* 2010;12:235–241.
34. Prasanna PG, Stone HB, Wong RS, et al. Normal tissue protection for improving radiotherapy: where are the gaps? *Transl Cancer Res* 2012;1:35–48.
35. Lee YW, Lee WH. Protective effects of genistein on proinflammatory pathways in human brain microvascular endothelial cells. *J Nutr Biochem* 2008;19:819–825.
36. Chacko BK, Chandler RT, Mundhekar A, et al. Revealing anti-inflammatory mechanisms of soy isoflavones by flow: modulation of leukocyte-endothelial cell interactions. *Am J Physiol Heart Circ Physiol* 2005;289:H908–H915.
37. Ahn GO, Tseng D, Liao CH, Dorie MJ, Czechowicz A, Brown JM. Inhibition of Mac-1 (CD11b/CD18) enhances tumor response to radiation by reducing myeloid cell recruitment. *Proc Natl Acad Sci U S A* 2010;107:8363–8368.
38. Cappuccini F, Eldh T, Bruder D, et al. New insights into the molecular pathology of radiation-induced pneumopathy. *Radiother Oncol* 2011;101:86–92.
39. Chiang CS, Liu WC, Jung SM, et al. Compartmental responses after thoracic irradiation of mice: strain differences. *Int J Radiat Oncol Biol Phys* 2005;62:862–871.
40. Zaynagetdinov R, Sherrill TP, Kendall PL, et al. Identification of myeloid cell subsets in murine lungs using flow cytometry. *Am J Respir Cell Mol Biol* 2013;49:180–189.
41. Laskin DL, Weinberger B, Laskin JD. Functional heterogeneity in liver and lung macrophages. *J Leukoc Biol* 2001;70:163–170.

42. Franke-Ullmann G, Pförtner C, Walter P, Steinmüller C, Lohmann-Matthes ML, Kobzik L. Characterization of murine lung interstitial macrophages in comparison with alveolar macrophages in vitro. *J Immunol* 1996;157:3097–3104.
43. Mosser DM, Edwards JP. Exploring the full spectrum of macrophage activation. *Nat Rev Immunol* 2008;8:958–969.
44. Gordon S, Taylor PR. Monocyte and macrophage heterogeneity. *Nat Rev Immunol* 2005;5:953–964.
45. Wu G, Morris SM Jr. Arginine metabolism: nitric oxide and beyond. *Biochem J* 1998;336 (Pt 1):1–17.
46. Laskin DL, Sunil VR, Gardner CR, Laskin JD. Macrophages and tissue injury: agents of defense or destruction? *Annu Rev Pharmacol Toxicol* 2011;51:267–288.
47. Zhang H, Han G, Liu H, et al. The development of classically and alternatively activated macrophages has different effects on the varied stages of radiation-induced pulmonary injury in mice. *J Radiat Res* 2011;52:717–726.
48. Gordon S, Martinez FO. Alternative activation of macrophages: mechanism and functions. *Immunity* 2010;32:593–604.
49. Barbul A. Proline precursors to sustain mammalian collagen synthesis. *J Nutr* 2008;138:2021S–2024S.

Erratum

Increasing Physical Activity and Exercise in Lung Cancer

Reviewing Safety, Benefits, and Application: Erratum

In regard to our recent article published in Journal of Thoracic oncology (Increasing Physical Activity and Exercise in Lung Cancer: Reviewing Safety, Benefits, and Application), we recognized an error that needs amending.[1]

In the "How Much Exercise" section, we suggest that the physical activity recommendation by the American Heart Association (150 min/wk of moderate intensity exercise)[1] is probably unattainable for most lung cancer patients. We cited Maddocks et al.'s[2] 2012 Letter to the Editor, "When will I get my breath back? Recovery time of exercise-induced breathlessness in patients with thoracic cancer." The letter reported that lung cancer and mesothelioma patients have a median relief of breathlessness after 4 minutes using an Incremental Shuttle Walk Test (median of 360 m over a mean of 373 sec). We erroneously stated that lung cancer patients exercised 4 minutes before they became breathless.

Despite our inaccurate reference to Maddocks et al.'s[2] letter, we still feel that exercise goals for healthy patients are unrealistic for most lung cancer patients. In 52 patients with lung cancer or mesothelioma after chemotherapy or radiotherapy, O'Driscoll et al.[3] reported that 50% reported breathlessness with walking, 19% reported breathlessness with bathing, and 17% reported breathlessness with bending or talking. Granger at al.[4] have shown that at diagnosis non–small-cell lung cancer patients engage in less physical activity than their healthy counterparts, and 6-minute walk distance (6MWD) in lung cancer patients is lower than in healthy patients. Whereas healthy adult 6MWD is estimated at 630 m,[5] and in 56 lung cancer patients, Granger et al.[4] reported mean 6MWD of 421 m with a minimal important difference between 22 and 42 m.

We still feel that physical activity is a safe and beneficial therapy for lung cancer. We apologize for our error.

References

1. Bade BC, Thomas DD, Scott JB, Silvestri GA. Increasing physical activity and exercise in lung cancer: reviewing safety, benefits, and application. *J Thorac Oncol* 2015;10:861–871.
2. Maddocks M, Taylor V, Klezlova R, England R, Manderson C, Wilcock A. When will I get my breath back? Recovery time of exercise-induced breathlessness in patients with thoracic cancer. *Lung Cancer* 2012;76:128–129.
3. O'Driscoll M, Corner J, Bailey C. The experience of breathlessness in lung cancer. *Eur J Cancer Care (Engl)* 1999;8:37–43.
4. Granger CL, Holland AE, Gordon IR, Denehy L. Minimal important difference of the 6-minute walk distance in lung cancer. *Chron Respir Dis* 2015;12:146–154.
5. ATS Committee on Proficiency Standards for Clinical Pulmonary Function Laboratories. ATS statement: guidelines for the six-minute walk test. *Am J Respir Crit Care Med* 2002; 166:111–117.